Mon. Not. R. Astron. Soc. **000**, 000–000 (0000) Printed 16 April 2013 (MN LATEX style file v2.2)

Mining the Aql X-1 long term X–ray light curve

S. Campana[1,⋆], F. Coti Zelati[1,2], P. D'Avanzo[1]
[1] *INAF-Osservatorio astronomico di Brera, Via Bianchi 46, I–23807, Merate (LC), Italy*
[2] *Università di Milano-Bicocca, Piazza della Scienza 3, I–20126 Milano, Italy*

16 April 2013

ABSTRACT
Aql X-1 is the prototypical low mass X–ray binary transient. The Rossi X–ray Timing Explorer All Sky Monitor provided a ~ 16 yr coverage revealing 20 outbursts. This is by far the most extensive legacy of outbursts from the same source. We investigated the outbursts characteristics in terms of energetics, peak luminosities, durations, decays and recurrence times. We found that bright outbursts (peak luminosity $\gtrsim 10^{37}$ erg s^{-1}) equal in number dimmer outbursts ($\lesssim 10^{36.6}$ erg s^{-1}). The peak luminosity does not correlate with outburst energetics, durations or quiescent times. We analysed the latest stages of the outbursts searching for exponential and/or linear decays. Light curve modeling led to constraints on the outer disk radius and enabled us to estimate the viscosity and the irradiation parameters. The former is larger than what has been obtained for other, shorter orbital period, transients, while the latter is somewhat smaller. This might be related to the longer orbital period of Aql X-1 with respect to other transient X–ray binaries.

Key words: Stars: individual: Aql X-1 – X–rays: binaries — binaries: close — accretion disc — stars: neutron

1 INTRODUCTION

Aql X-1 is the most prolific neutron star low mass X–ray binary transient (LMXTs). Seven outbursts were observed by the *Vela 5B* satellite between 1969–1976 (Priedhorsky & Terrell 1984). The *Ariel 5* satellite detected three outbursts in the 1976–1979 time period. Three more outbursts were detected by the All-Sky Monitor (ASM) on board the *Ginga* satellite in the 1987–1992 time frame (Kitamoto et al. 1993). Despite this high number of events, the sky coverage was not complete and some outbursts might have been lost. Interestingly, the recurrence period of the outbursts was short in the seventies, around 125 d (Priedhorsky & Terrell 1984), but it became longer in the eighties, around 300 d (Kitamoto et al. 1993).

The Rossi X–ray Timing Explorer (*RXTE*, 1996–2012, Levine et al. 1996) and more recently the Monitor All-sky X–ray Image (*MAXI*, 2009–now, Matsuoka et al. 2009) All-sky Monitors are continuously surveying with higher sensitivity the X–ray sky. Up to Sept. 2011, the *RXTE*/ASM detected twenty outbursts from Aql X-1 (two in common with *MAXI*). These data provide a unique database for investigations on outburst recurrence times and energetics.

The limiting sensitivity of *RXTE*/ASM is such that in the case of Aql X-1 we can follow the outburst decay down to a 2–10 keV luminosity of $\sim 5\times10^{35}$ erg s^{-1} (at a distance of 5 kpc; Jonker & Nelemans 2004). In the case of *MAXI* we can reach a somewhat better (within a factor of two) limiting sensitivity. In addition to the possibility of detecting faint outbursts, this luminosity is sufficiently faint to allow us to investigate the outburst's decay law. King & Ritter (1998) showed that X–ray heating during the decay from an outburst causes the light curves of LMXTs to show either exponential or linear decays, depending on whether or not the X–ray luminosity is sufficiently high to keep the outer disc edge hot. The rationale behind this is that if the disc's outer portion is hot the entire disc is hot and matter can be efficiently transferred to the compact object, delivering a fast drain of the accretion disc.

In this paper we exploit the *RXTE*/ASM (and *MAXI*) database on Aql X-1. In Section 2 we discuss the data and characterise the outbursts. In Section 3 we focus on correlations among outburst properties and we fit the decay profiles of the outbursts to derive the outer disc radius (Section 4). In Section 5 we discuss our results.

2 DATA ANALYSIS

2.1 *RXTE* data

The *RXTE*/ASM consisted of three position-sensitive Scanning Shadow Cameras (Levine et al. 1996). *RXTE* started operating in Jan. 1996. The satellite was slowly spinning, observing sources for 90 s (dwell) during the 96 min duration of

⋆ E-mail: sergio.campana@brera.inaf.it

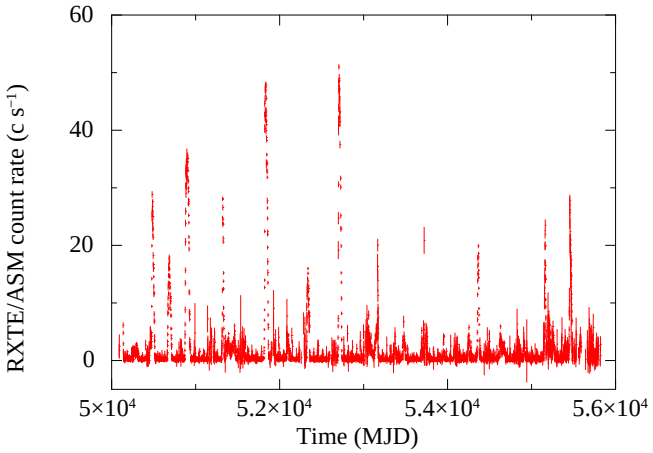

Figure 1. *RXTE*/ASM light curve of Aql X-1. Data are one day averages and report the ASM rate in the 1.5–12 keV energy band. Data have been filtered in order to get rid of negative values ($\sim$ 28% of the data). For comparison the Crab nebula provides 75 count s^{-1}.

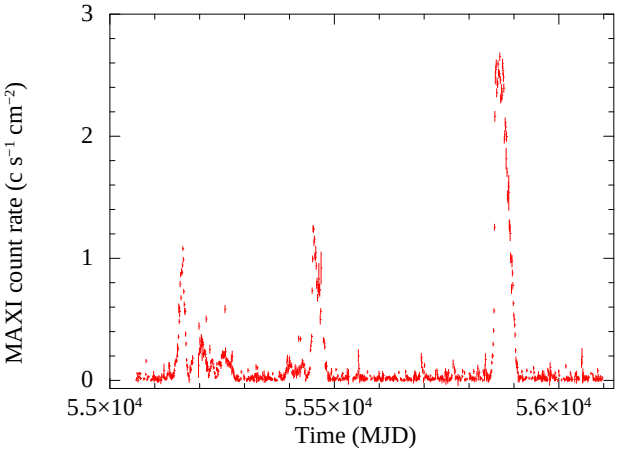

Figure 2. *MAXI* light curve of Aql X-1. Data are one day averages in the 2–20 keV energy band. Data have been filtered in order to get rid of negative values ($\sim$ 20% of the data). For comparison the Crab nebula provides 3.5 count s^{-1} cm^{-2}.

each orbit. Raw data points provided the fitted source rates in the 1.5–12 keV energy band from one dwell. One-day averages are more commonly used, resulting from the average of the fitted source rates from the dwells during that time interval (typically 5-10). Each measurement (count rate) has an error associated, coming from the quadrature average of the estimated errors on the individual dwells. The one-day average light curve of Aql X-1 is shown in Fig. 1 (the flux of the Crab is $\sim$ 75 count s^{-1}).

2.2 *MAXI* data

The *MAXI* is a position-sensitive X–ray all-sky monitor instrument, to scan almost the entire sky during its orbit, once every 96 minutes (Matsuoka et al. 2009). *MAXI* is located on the International Space Station and is collecting data since Aug. 2009. The detection sensitivity is somewhat

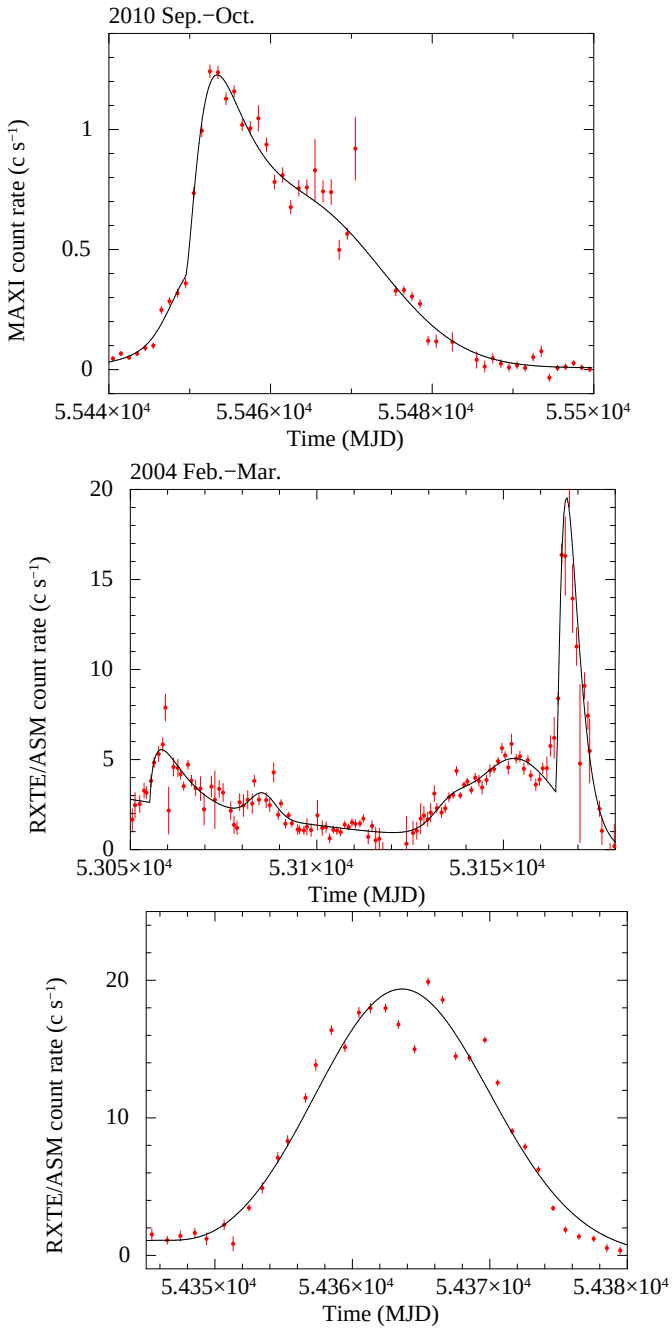

Figure 3. Examples of outburst fitting. From top to bottom are shown the Aql X-1 outburst of 2010 Sep-Oct (*MAXI*, FRED), 2004 Feb-Mar (*RXTE*, LIS-FRED) and 2007 Sep (*RXTE*, Gaus).

better than *RXTE*/ASM, reaching a few mCrab during one day observations. The operational energy range is 2–20 keV. The one-day average light curve of Aql X-1 is shown in Fig. 2 (the flux of the Crab is $\sim$ 3.5 count s^{-1} cm^{-2}).

3 OUTBURST ANALYSIS

During the Jan 1996 – Sep 2011 time interval 20 outbursts from Aql X-1 were recorded by *RXTE* and *MAXI*. Usually

Table 1. Aql X-1 outbursts.

Outburst	Morphology	Duration (d)	Day Peak (MJD)	Rate peak (mCrab)	Rise (d)	Decay (d)	Quiescent time* (d)	Energy (10^{42} erg)
1996 Feb	FRED	9	50136	87	1	8	–	1.1
1996 May-Aug	Multi-peak	95	50298	38	15	21	81	7.6
1997 Jan-Mar	LIS-FRED-P	90	50483	379	8	30	120	21.7
1997 Aug-Sep	Gaus-P	64	50684	220	28	36	126	12.6
1998 Feb-May	Multi-peak	85	50885	482	19	40	145	27.6
1999 May-Nov	FRED-P-LIS	184	51320	376	12	172	358	21.5
2000 Sep-Nov	FRED-P	58	51841	628	12	28	318	36.0
2001 Jun-Aug	Multi-peak	58	52087	65	16	42	203	3.7
2002 Feb-Apr	FRED-P	60	52337	209	27	33	181	12.0
2003 Feb-Apr	FRED	64	52706	649	20	44	316	37.1
2004 Feb-Jun	LIS-FRED	130	53167	259	8	13	300	14.8
2005 Mar-May	FRED-P	70	53473	66	23	47	270	3.8
2005 Nov	FRED	24	53692	68	6	12	160	3.9
2006 Jul-Aug	FRED-P	40	53952	57	7	16	236	3.3
2007 May-Jun	Multi-peak	54	54254	64	24	30	250	3.7
2007 Sep	Gaus	36	54364	257	24	12	56	14.7
2008 May-Jun	FRED-P	150	54627	55	32	73	174	3.1
2009 Mar-Apr	FRED	40	54906	44	6	34	200	2.5
2009 Nov-Dec	Gaus-P	38	55163	311	23	15	200	24.9
2010 Sep-Oct	FRED	60	55453	349	13	47	262	27.8

* Quiescent time before the start of the outburst.

the morphology of LMXTs is characterised by a fast rise and an exponential decay shape (Chen et al. 1997). In systems like Aql X-1, i.e. neutron star X–ray binary transients, the thermal viscous disc instability model (DIM; Lasota 2001) is usually considered to explain the transient behaviour. However, it has been shown that the DIM alone cannot reproduce FRED-like outbursts. The other key ingredient is X–ray irradiation. The irradiation of the outer parts of the accretion disc is caused by the intense X–ray flux produced from the innermost disc regions and from the neutron star itself. Irradiation dominates and heavily changes the outer disc temperature profile.

X–ray irradiation is also responsible for the decay of the outburst. If the outer disc edge is kept hot (i.e. above the temperature of the DIM hot viscous state), accretion disc theory predicts an exponential decay for the outburst (King & Ritter 1998). On the contrary if (or when) disc irradiation is not strong enough, the outer disc edge temperature falls below the limiting hot temperature of the DIM, and we can expect a linear decay of the X–ray flux.

We have analysed and characterised all the 20 Aql X-1 outbursts observed by *RXTE*/ASM. For each one of them we have first classified the outbursts, following Maitra & Baylin (2008). Outbursts were classified based on their X–ray morphology as: *i*) Fast Rise Exponential Decay (FRED); *ii*) FRED with peak(s): when overlaid to the FRED morphology there are pronounced peaks; *iii*) multi-peaks: when the presence of many peaks distorts the overall morphology; *iv*) Gaussian (Gaus): when the rise and decay times are more similar. The typical observed (*e*-folding) FRED rise times are approximately few days (up to a week) and the decay times are 3–4 weeks. According to Wachter et al. (2002), we observe that usually, following an outburst (but sometimes also preceding an outburst), the source might remain stuck in a low-intensity state (LIS), before ending (starting) the outburst. Outbursts are classified according to this scheme in Table 1. A few examples are shown in Fig. 3.

We then investigated outburst characteristic times. The duration of an outburst is simply computed as the time difference between the first and last detection of a given outburst detected by the *RXTE*/ASM or *MAXI* (the latest two, see Table 1). The day of the outburst peak is reported in Table 1. We also consider rise and decay times. In order to be model independent, we prefer to separately indicate the time needed to reach the outburst peak (rise) and the time needed to reach non-detection (decay). In the case of a typical FRED-like (or Gaussian-like) outburst, the sum of the rise and decay times gives the outburst duration time. This is not the case when other main peaks are present or when there is a LIS.

We fitted each outburst profile with simple models in order to get a description of their overall shapes. A few of them are shown in Fig. 3. It is clear that outbursts can be very complicated and the analytical description does not provide a detailed account of all the small variations observed in the light curve. For this reason the reduced χ^2 obtained from the fit are often much larger than unity. Despite this, we verified that the overall fit we considered is able to account for the total energetics of the outbursts to a $\sim 10\%$ precision (this has been done for a few outburst cases, integrating point by point the light curve and extrapolating the data when observations were missing and comparing the results with the integral of the analytical function). To derive the outburst energetics we simply assumed a Crab-like spectrum. Knowing the source distance (5 kpc) and the column density ($N_H \sim (3-4) \times 10^{21}$ cm^{-2}, e.g. Sakurai et al. 2012), one can convert count rates into luminosities.

4 OUTER DISC RADIUS ESTIMATE

The late-stage light curve of LMXT outbursts are often characterised in terms of exponential or linear decays. If the outer disc edge is kept hot (i.e. above the temperature of the DIM hot viscous state), accretion disc theory predicts an exponential decay for the outburst, otherwise the decay is predicted to be linear (King & Ritter 1998). King & Ritter (1998) noticed that the exponential decay must revert to the linear mode when the X–ray flux has decreased sufficiently, but did not analyse this in detail. Powell, Haswell & Falanga (2007) took into account the continuous mass transfer into the disk from the donor star, and rewrote the total central mass accretion rate equation for the decay outburst profiles. When the maximum disk radius of the hot viscous portion of the disk, R_h, becomes smaller than the total disk radius, $R_{\rm disk}$, (i.e. when the outer part of the disk is no longer kept in the hot, viscous state by central irradiation), then R_h will decrease linearly and, correspondingly the X–ray luminosity will turn from an exponential to a linear decay. When this occurs a distinctive knee in the light curve outburst decay can be expected (see also Shahbaz, Charles & King 1998).

At variance with the above outburst light curve fits, here we fit all the latest stages of Aql X-1 outbursts with a function

$$N = (N_t - N_e)\exp\left(-\frac{t-t_t}{\tau_e}\right) + N_e \qquad (1)$$

for the exponential part, where N_e is the count rate corresponding to the limit of the exponential decay, N_t is the count rate at the knee, and τ_e is the time-scale of the exponential decay. The linear decline is given by:

$$N = N_t\left(1 - \frac{t-t_t}{\tau_l}\right), \qquad (2)$$

where τ_l is the time after the knee at which the (extrapolated) count rate goes to zero. The two functions join at the exponential/linear transition knee. This function fully exploits Powell et al. (2007) outburst decay theory. Based on a Crab-like spectrum, one can convert rates into luminosities and relate the outburst decay to physical quantities of the system. An example is shown in Fig. 4.

The rate N_t can be converted into a luminosity L_t and related to the outer disc radius as $L_t = R_{\rm disc}(L_t)^2/\Phi$, where Φ is a constant related to the disc irradiation properties. Current estimates of Φ are in the range $(1-9)\times10^{-15}$ cm^2 s erg^{-1} (see Eq. 2 in Powell et al. 2007 and King & Ritter 1998). A different estimate of the outer disc radius comes from the exponential decay time. This is related to the radius as $\tau_e = \frac{R_{\rm disc}(\tau_e)^2}{3\,\nu}$, where ν is the viscosity at the outer disc edge. An estimate of the viscosity parameter ν is in the range $(4-10)\times10^{14}$ cm^2 s^{-1} (Powell et al. 2007; King & Ritter 1998).

Additional constraints on the outer disc boundary come from the fact that it must be larger than the circularisation radius (the radius at which matter in Keplerian orbit has the same angular momentum as at the first Lagrangian point) and smaller than the first Lagrangian point from the center of the primary. In the case of Aql X-1 with an orbital period of 18.97 hr (Welsh, Robinson &Young 2000), the circularisation radius is $R_{\rm circ} \sim 5.0\times10^{10}$ cm (assuming a mass ratio of 0.3) and the distance of the first Lagrangian point from the center of the primary is $b_1 = 2.0\times10^{11}$ cm (Frank, King & Raine 2002).

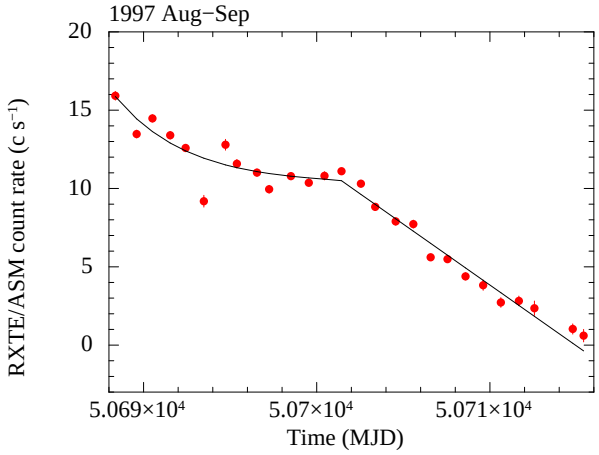

Figure 4. Example of a fit with an exponential and linear function of the 1997 Aug-Sep outburst from Aql X-1 (*RXTE*/ASM data). The two curves join at the exponential knee.

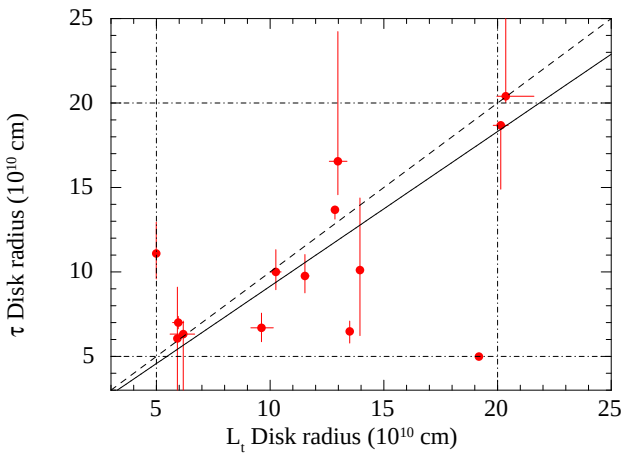

Figure 5. Outer disc radius estimate based on the knee luminosity at the exponential/linear transition (x axis) and on the exponential decay time (y axis). Horizontal and vertical dot-dashed lines mark the circularisation radius (smaller) and the distance between the neutron star and the inner Lagrangian point (larger). The dashed line indicates the equality among the two radii, whereas the continuous line is the best fit line.

Adopting the values usually reported in the literature for ν and Φ, the outer disc radius is smaller than circularisation radius. Imposing the condition that $R_{\rm disc}(\tau_e)$ is larger than the circularisation radius, we can infer that $\nu \gtrsim 9\times10^{15}$ cm^2 s^{-1} for all radii derived from the exponential decay. Using this value for ν all the derived radii are also smaller than the b_1 radius, consistent with expectations (see Fig. 5). The same constraint can be applied to the luminosity radius $R_{\rm disc}(L_t)$. In this case we derive $\Phi \lesssim 8\times10^{-16}$ cm^2 s erg^{-1}. Again, imposing this value, all the radii are also consistent to be smaller than the b_1 radius (see Fig. 5).

Assuming these values for ν and Φ one can compare the two determinations of the radii with the two methods finding a relatively good agreement, with only a few outliers. Overall

Table 2. Aql X-1 outburst decay fits.

Outburst	Time interval (MJD)	N_t (c s^{-1})	N_e (c s^{-1})	τ_e (d)	$R_{\rm disc}(L_t)$ (10^{10} cm)	$R_{\rm disc}(\tau_e)$ (10^{10} cm)
1996 Feb	too few points	–	–	–	–	–
1996 May-Aug	too few points	–	–	–	–	–
1997 Jan-Mar	50503–50522	$15.4^{+0.3}_{-0.2}$	$14.5^{+0.1}_{-3.5}$	$4.5^{+4.6}_{-2.8}$	$14.0^{+0.1}_{-0.1}$	$10.1^{+4.3}_{-3.9}$
1997 Aug-Sep	50708–50719	$10.5^{+0.3}_{-0.3}$	$10.6^{+0.7}_{-0.9}$	$4.2^{+1.2}_{-0.8}$	$11.5^{+0.2}_{-0.2}$	$9.8^{+1.3}_{-1.0}$
1998 Feb-May	50922–50949	$29.2^{+0.2}_{-0.2}$	$29.2^{+0.2}_{-0.2}$	$1.1^{+0.1}_{-0.1}$	$19.2^{+0.1}_{-0.1}$	$5.0^{+0.1}_{-0.1}$
1999 May-Nov	51330–51347	$13.1^{+0.3}_{-0.3}$	$0.0^{+2.5}_{-0.0}$	$8.2^{+0.2}_{-0.7}$	$12.9^{+0.1}_{-0.2}$	$13.7^{+0.2}_{-0.6}$
2000 Sep-Nov	51857–51875	$32.1^{+1.1}_{-1.0}$	$19.9^{+0.0}_{-0.1}$	$15.3^{+0.1}_{-5.6}$	$20.1^{+0.3}_{-0.3}$	$18.7^{+0.1}_{-3.8}$
2001 Jun-Aug	too few points	–	–	–	–	–
2002 Feb-Apr	52354–52367	$8.3^{+0.4}_{-0.4}$	$8.0^{+0.5}_{-0.8}$	$4.4^{+1.2}_{-0.9}$	$10.3^{+0.2}_{-0.3}$	$10.0^{+1.3}_{-1.1}$
2003 Feb-Apr	52730–52747	$32.8^{+4.1}_{-1.3}$	$0.0^{+20.2}_{-0.0}$	$18.2^{+20.4}_{-0.7}$	$20.4^{+1.2}_{-0.4}$	$20.4^{+9.3}_{-0.4}$
2004 Feb-Jun	53171–53180	$7.3^{+0.8}_{-0.7}$	$6.1^{+0.1}_{-3.7}$	$2.0^{+0.5}_{-0.5}$	$9.6^{+0.5}_{-0.5}$	$7.0^{+0.9}_{-0.8}$
2005 Mar-May	53494–53510	$2.8^{+0.1}_{-0.1}$	$2.8^{+0.1}_{-0.2}$	$1.6^{+2.0}_{-1.2}$	$5.9^{+0.1}_{-0.1}$	$6.1^{+3.0}_{-3.1}$
2005 Nov	53695–53704	$3.0^{+0.5}_{-0.5}$	$0.0^{+3.5}_{-0.0}$	$1.8^{+0.5}_{-1.6}$	$6.2^{+0.5}_{-0.6}$	$6.3^{+0.8}_{-4.4}$
2006 Jul-Aug	too few points	–	–	–	–	–
2007 May-Jun	too few points	–	–	–	–	–
2007 Sep	54370–54382	$14.4^{+0.3}_{-0.2}$	$13.8^{+0.4}_{-0.4}$	$1.8^{+0.4}_{-0.4}$	$13.5^{+0.1}_{-0.1}$	$6.5^{+0.6}_{-0.7}$
2008 May-Jun	54676–54690	$2.0^{+0.1}_{-0.1}$	$2.0^{+0.1}_{-0.2}$	$5.4^{+2.0}_{-1.4}$	$5.0^{+0.1}_{-0.1}$	$11.1^{+1.9}_{-1.5}$
2009 Mar-Apr	too few points	–	–	–	–	–
2009 Nov-Dec	55168–55177	$2.8^{+0.2}_{-0.2}$	$2.0^{+0.4}_{-0.4}$	$2.2^{+0.2}_{-0.2}$	$6.0^{+0.2}_{-0.3}$	$7.0^{+0.4}_{-0.4}$
2010 Sep-Oct	55472–55490	$13.4^{+0.8}_{-0.8}$	$9.1^{+1.2}_{-9.1}$	$12.0^{+13.7}_{-2.7}$	$13.0^{+0.4}_{-0.4}$	$16.6^{+7.7}_{-2.0}$

there is a factor of ~ 4 variation in the estimated outer disc radii among different outbursts. This can be due to (small) variations in the outer disc radius, outer disc viscosity, or irradiation parameter.

5 DISCUSSION AND CONCLUSIONS

The outbursts from Aql X-1 observed by *RXTE*/ASM span a long time interval (Jan 1996 – Sep 2011). Twenty outbursts were recorded. Outbursts occur mainly in the FRED flavour and often with secondary maxima (see Table 1). Peak luminosities can be divided into two separated groups: 11 outbursts fall within $10^{37} - 10^{37.6}$ erg s^{-1} and 9 within $10^{36.3} - 10^{36.6}$ erg s^{-1} with no outbursts in between (factor of ~ 3 luminosity gap). Ideally one would expect a correlation between the outburst peak luminosity and the recurrence time but this is not the case (see Fig. 6). In Fig. 6 we also included outbursts from *Vela 5B* and *Ariel 5* (Kitamoto et al. 1993). Due to the higher limiting fluxes of these instruments, all the old outbursts fall in the bright group. A weak correlation (4% probability, according to the Spearman rank test) is present among these two variables, including the *RXTE* outbursts and the *Vela 5B* and *Ariel 5* ones (see Fig. 6).

One can also expect a correlation among the peak outburst luminosity and the total energy of the outburst. This is not the case as shown in Fig. 7. According to a Spearman rank correlation test, there is 23% of a chance correlation. This is due to the presence of ~ 4 long-lasting low peak luminosity outbursts with a large emitted energy as well as ~ 1 short-duration high peak luminosity low energetic burst. This indicates that the peak outburst luminosity is not a good tracer of the outburst energetics.

We model the outburst decays with a combination of exponential and linear functions following Powell et al. (2007).

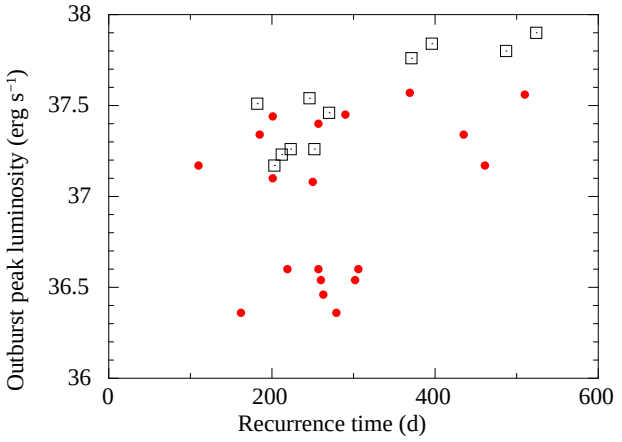

Figure 6. Outburst peak X–ray luminosity vs. recurrence time. Red filled circles refer to *RXTE/ASM* and *MAXI* data during the time interval 1996-2011 (this work). Black open squares refer to the time interval 1970-1979 (Kitamoto et al 1993).

A note of caution should be added since not all the low mass transient outbursts can be described by this model. A clear example is provided by the 2004 outburst from IGR J00291+5934 showing a bright outburst with a clear linear decay (Hartman, Galloway & Chakrabarty 2011).

Our modeling leads to two different estimates of the outer disc radius depending on the outer disc viscosity and on the outer disc irradiation properties. Imposing that the outer disc radius lies between the circularisation radius and the distance between the neutron star and the inner Lagrangian point, we can constrain these two parameters. In particular, we derive $\nu \gtrsim 9\times10^{15}$ cm^2 s^{-1} and $\Phi \lesssim 8\times10^{-16}$ cm^2 s erg^{-1}. The viscosity estimate is somewhat larger than

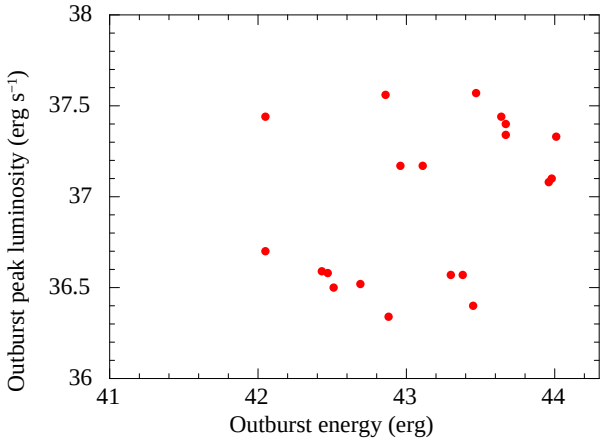

Figure 7. Outburst peak X–ray luminosity vs. total outburst energy. Red filled circles refer to *RXTE/ASM* and *MAXI* data during the time interval 1996-2011.

the value obtained by Powell et al. (2007). These authors found $\nu \sim 4 \times 10^{14}$ cm^2 s^{-1} (factor of ~ 20 smaller), considering short orbital period accreting millisecond pulsars. The value we derived is also somewhat larger than the one obtained by Shahbaz et al. (1998) for Aql X-1 (factor 3–5), based, however, on a simpler modeling. This might be related to the very long orbital period of Aql X-1, pushing the outer disc edge a factor of 10–100 out with respect to the systems considered by Powell et al. (2007). The only long orbital period system considered by Powell et al. (2007) is the bursting pulsar GRO J1744–28 ($P_{\rm orb} = 11.8$ d), which is indeed characterised by a factor of ~ 10 longer exponential decay time, confirming the increasing trend of the viscosity for larger accretion disk outer edges.

The irradiation parameter is instead lower than current estimates: $(4-9)\times10^{-15}$ cm^2 s erg^{-1} based on King & Ritter (1998) or 1.3×10^{-15} cm^2 s erg^{-1} on Powell et al. (2007). Our value is consistent with the latter estimate (just a factor of ~ 2 lower), whereas longer orbital period systems, such as GRO J1744–28, are characterised by $\Phi \sim 10^{-15} - 10^{-14}$ cm^2 s^{-1}, indicating that irradiation effects play minor role.

Adopting our values for ν and Φ we found a good agreement among the two different outer radii estimates based on the outburst decay light curve fitting. From Fig. 5 it is apparent that, for common values of ν and Φ, the outer radius can span a factor of ~ 4 variation among different outbursts.

Given our 20 yr baseline we can compute the mean mass accretion rate of Aql X-1, integrating the observed luminosity. The mean mass accretion rate is $\dot{M} \sim 7 \times 10^{15}$ g s^{-1} (assuming a standard 1.4 $M_\odot$ and 10 km neutron star). Given the 18.97 hr orbital period, this value places Aql X-1 well within the unstable region of the Disc Instability Model (Lasota 2001).

Finally, we estimated a mean recurrence time for the system of 280 ± 103 d ($1\,\sigma$). This is considerably longer than the early recurrence time (~ 125 d) estimated by Priedorsky & Terrell (1984) and more in line with the estimate of ~ 300 d by Kitamoto et al. (1993; see also Šimon 2002). We also note that dim outbursts (those with a peak luminosity lower than $10^{36.6}$ erg s^{-1}) are more regular with a recurrence of 256 ± 47 d (18% dispersion). With a frequency of 1.36 outbursts per year in the *RXTE* era, Aql X-1 is the most prolific neutron star transient in the Galaxy.

6 ACKNOWLEDGMENTS

We thank the referee for useful comments and suggestions. We thank Andrea Melandri for comments.

REFERENCES

Chen, W., Shrader, C. R., Livio M. 1997 ApJ, 491, 312
Frank, J., King, A. R., Raine, D. J. 2002, Accretion Power in Astrophysics. Cambridge University Press, Cambridge, UK
Hartman, J. M., Galloway, D. K., Chakrabarty, D. 2011, ApJ, 726, 26
Jonker, P. G., Nelemans, G. 2004, MNRAS, 354, 355
King, A. R., Ritter H. 1998, MNRAS, 293, L42
Kitamoto, S., Tsunemi, H., Miyamoto, S., Roussel-Dupre, D. 1993, ApJ, 403, 315
Lasota, J.-P. 2001, NewAR, 45, 449
Levine, A. M., et al. 1996, ApJ, 469, L33
Maitra, D., Bailyn, C. D. 2008, ApJ, 688, 537
Matsuoka, M., et al. 2009, PASJ, 61, 999
Powell, C. R., Haswell, C. A., Falanga, M. 2007, MNRAS, 374, 466
Priedhorsky, W. C., Terrell, J. 1984, ApJ, 280, 661
Sakurai, S., et al. 2012, PASJ, 64, 72
Shahbaz, T., Charles, P. A., King, A. R. 1998, MNRAS, 301, 382
Šimon, V. 2002, ASPC, 261, 549
Wachter, S., Hoard, D. W., Bailyn, C. D., Corbel, S., Kaaret, P. 2002, ApJ, 568, 901
Welsh, W. F., Robinson, E. L., Young, P. 2000, AJ, 120, 943